Cell Reports, Volume *42*

Supplemental information

High-calorie diets uncouple hypothalamic oxytocin neurons from a gut-to-brain satiation pathway via κ-opioid signaling

Tim Gruber, Franziska Lechner, Cahuê Murat, Raian E. Contreras, Eva Sanchez-Quant, Viktorian Miok, Konstantinos Makris, Ophélia Le Thuc, Ismael González-García, Elena García-Clave, Ferdinand Althammer, Quirin Krabichler, Lisa M. DeCamp, Russell G. Jones, Dominik Lutter, Rhiannan H. Williams, Paul T. Pfluger, Timo D. Müller, Stephen C. Woods, John Andrew Pospisilik, Celia P. Martinez-Jimenez, Matthias H. Tschöp, Valery Grinevich, and Cristina García-Cáceres

Figure S1

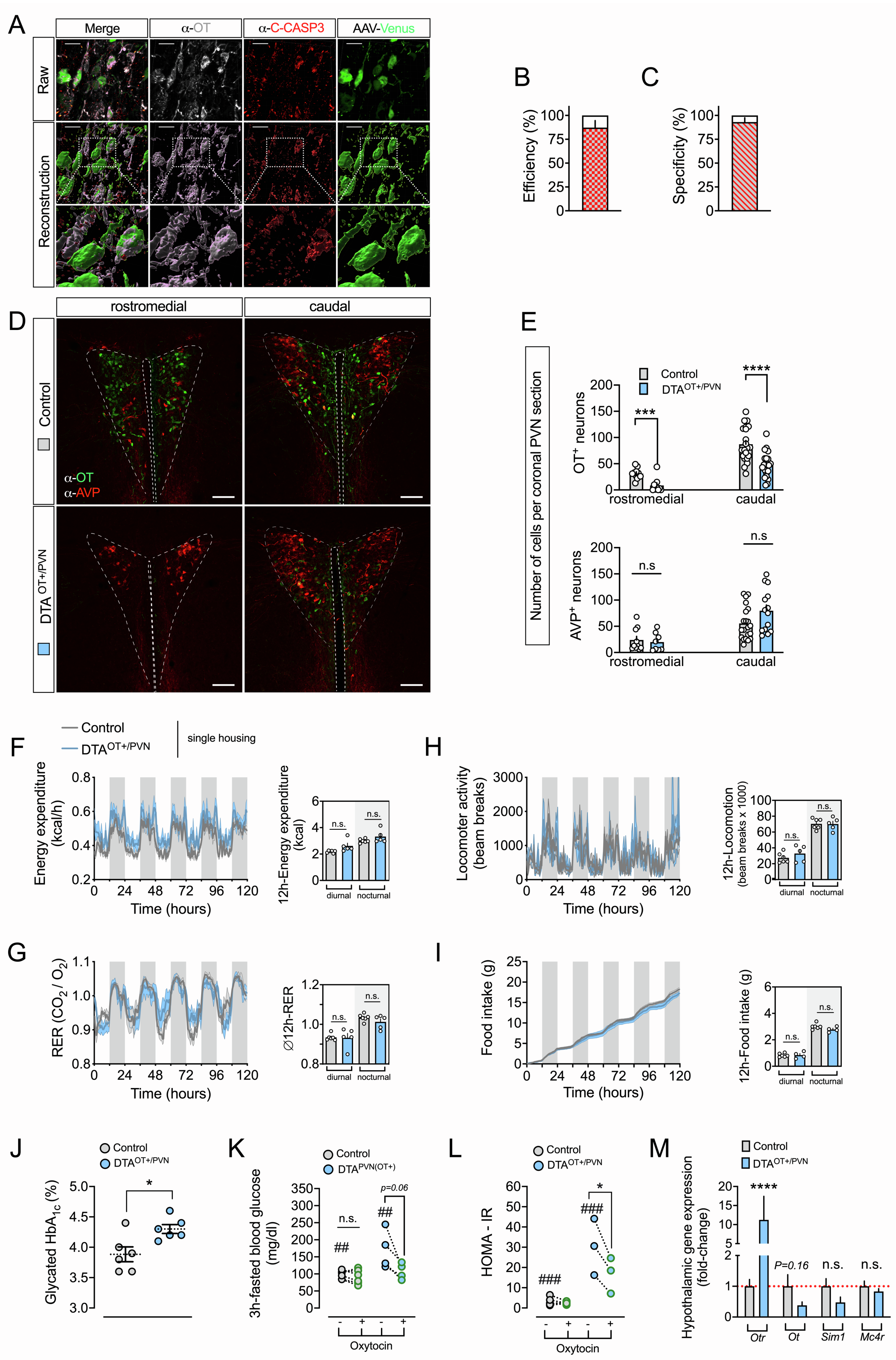

A
Merge
α-OT
α-C-CASP3
AAV-Venus
Raw
Reconstruction
B
Efficiency (%)
C
Specificity (%)
D
rostromedial
caudal
Control
DTA OT+/PVN
α-OT
α-AVP
E
Number of cells per coronal PVN section
Control
DTA OT+/PVN
OT+ neurons
AVP+ neurons
rostromedial
caudal
n.s
F
Control
DTA OT+/PVN
single housing
Energy expenditure (kcal/h)
Time (hours)
12h-Energy expenditure (kcal)
diurnal
nocturnal
n.s.
G
RER (CO2 / O2)
Ø12h-RER
H
Locomoter activity (beam breaks)
12h-Locomotion (beam breaks x 1000)
I
Food intake (g)
12h-Food intake (g)
J
Glycated HbA1c (%)
K
DTA PVN(OT+)
3h-fasted blood glucose (mg/dl)
p=0.06
Oxytocin
L
HOMA - IR
M
Hypothalamic gene expression (fold-change)
P=0.16
Otr
Ot
Sim1
Mc4r

Figure S1. Related to Figure 1: Virus-mediated ablation of PVN^{OT} neurons induces hyperphagic obesity that is rectifiable by exogenous oxytocin treatment and associated with CCK resistance.

(A) Representative, 3D rendered confocal micrographs of $DTA^{OT+/PVN}$ mice showing pro-apoptotic PVN^{OT} neurons 5 days after AAV injections. C-CASP3 immunoreactivity (red) co-localizes with the majority of OT^+ (gray) and AAV-$Venus^+$ (green) neurons, but not with neighboring cells as indicated in the raw images (upper panel), the reconstructed images (middle panel), and the reconstructed magnified insert (lower panel). Scale bar, 20 μm.

(B) Corresponding quantification of ablation efficiency presented as percentage of all OT^+ neurons (gray) also expressing C-CASP3 (red). n = 5 mice, 543 neurons.

(C) Corresponding quantification of ablation specificity presented as percentage of all C-$CASP3^=$ cells (red) also expressing OT (gray). n = 5 mice, 543 neurons.

(D) Representative confocal micrographs of brain sections showing OT^+ neurons (green) and AVP^+ neurons (red) of control mice and $DTA^{OT+/PVN}$ mice at the rostromedial and caudal levels of the PVN. Scale bar, 100 μm.

(E) Corresponding quantification of OT neuron count (upper panel) and AVP neuron count (lower panel) control mice and $DTA^{OT+/PVN}$ mice at the rostromedial and caudal levels. n = 5-7, 3-5 hemisections per mouse.

(F) Hourly energy expenditure as measured by indirect calorimetry in metabolic cages of single-housed control mice and $DTA^{OT+/PVN}$ mice (left panel) as well as average 12h-energy expenditure (right panel). Data are presented as mean ± SEM. ** P < 0.01, **** P < 0.0001. n = 5-7 mice (two-way ANOVA (left panel) and unpaired Student's *t*-test (right panel).

(G) Hourly respiratory exchange ratio (RER) as measured by indirect calorimetry in metabolic cages of single-housed control mice and $DTA^{OT+/PVN}$ mice (left panel) as well as average 12h-RER (right panel). Data are presented as mean ± SEM. n.s., not significant. n = 5-7 mice (two-way ANOVA (left panel) and unpaired Student's *t*-test (right panel)).

(H) Hourly locomotor activity as measured by beam breaks in metabolic cages of single-housed control mice and $DTA^{OT+/PVN}$ mice (left panel) as well as average 12h-locomotion (right panel). Data are presented as mean ± SEM. n.s., not significant. n = 5-7 mice (two-way ANOVA (left panel) and unpaired Student's *t*-test (right panel)).

(I) Cumulative food intake of single-housed control mice and $DTA^{OT+/PVN}$ mice (left panel) as well as average 12h-food intake (right panel). Data are presented as mean ± SEM. n.s., not significant. n = 5-7 mice (two-way ANOVA (left panel) and unpaired Student's *t*-test (right panel)).

(J) Quantification of glycated HbA_{1C} in a separate cohort of $DTA^{OT+/PVN}$ mice and control mice. Data are presented as mean ± SEM. n.s., not significant. * P < 0.05. n = 6 mice (unpaired Student's *t*-test).

(K) Quantification of 3h-fasted blood glucose before and after treatment with bi-daily OT (500 nmol/kg BW; *s.c.*) in $DTA^{OT+/PVN}$ mice and control mice. Data are presented as mean ± SEM. ## P < 0.01, n.s., not significant. n = 5-7 mice (one-way ANOVA and paired Student's *t*-test).

(L) Quantification of HOMA-IR before and after treatment with bi-daily OT (500 nmol/kg BW; *s.c.*) in $DTA^{OT+/PVN}$ mice and control mice. Data are presented as mean ± SEM. * P < 0.05, ### P < 0.001, n.s., not significant. n = 5-7 mice (one-way ANOVA and paired Student's *t*-test).

(M) Relative gene expression of mRNA for *Otr*, *Ot*, *Sim1* and *Mc4r* in the hypothalamus of $DTA^{OT+/PVN}$ mice normalized to control mice. Data are presented as mean ± SEM. * P < 0.05, n.s., not significant. n = 4 mice (unpaired Student's *t*-test).

Figure S2

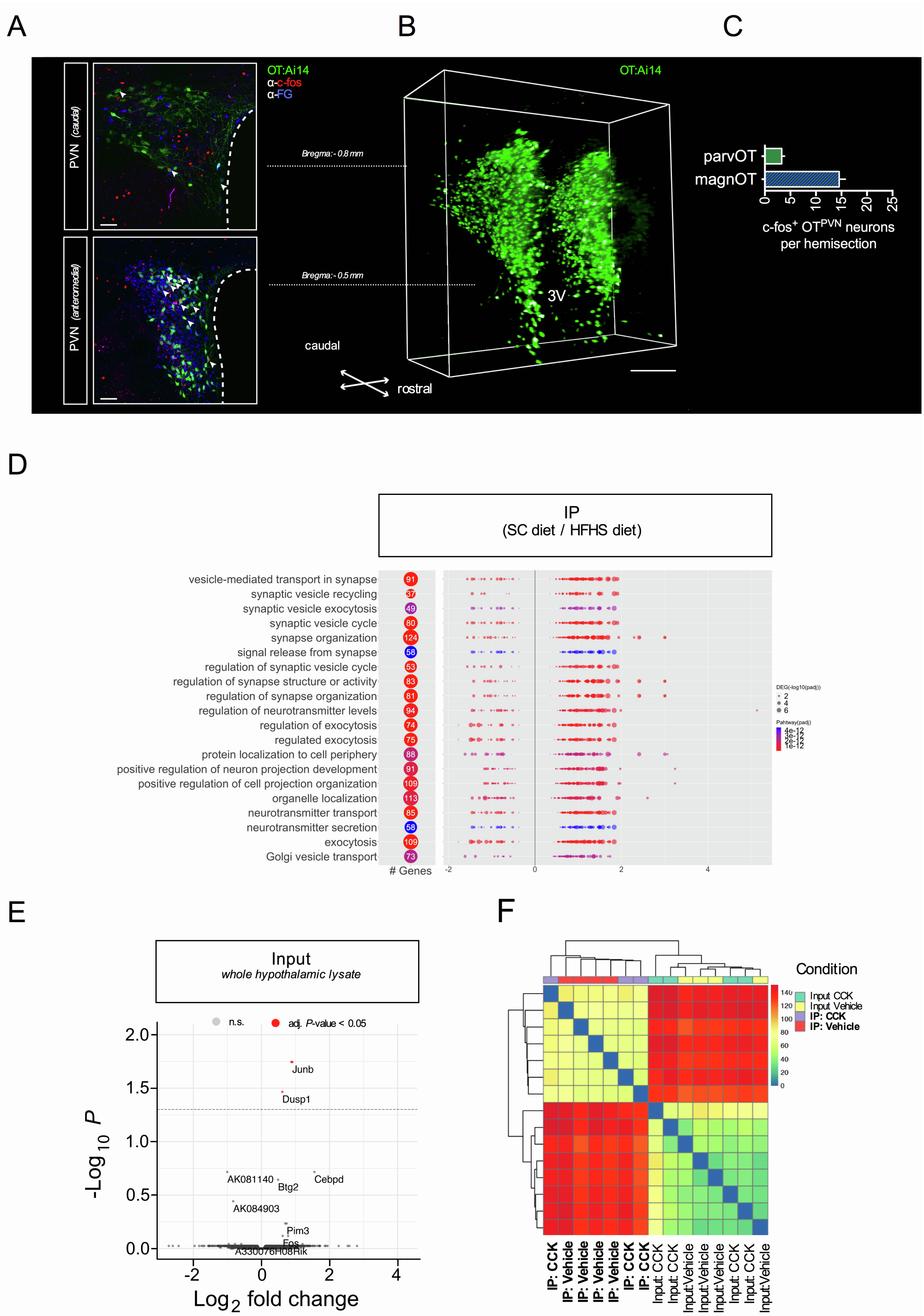
A
B
C
OT:Ai14
α-c-fos
α-FG
PVN (caudal)
PVN (anteromedial)
Bregma: - 0.8 mm
Bregma: - 0.5 mm
caudal
rostral
3V
parvOT
magnOT
0 5 10 15 20 25
c-fos+ OTPVN neurons per hemisection
D
IP
(SC diet / HFHS diet)
vesicle-mediated transport in synapse
synaptic vesicle recycling
synaptic vesicle exocytosis
synaptic vesicle cycle
synapse organization
signal release from synapse
regulation of synaptic vesicle cycle
regulation of synapse structure or activity
regulation of synapse organization
regulation of neurotransmitter levels
regulation of exocytosis
regulated exocytosis
protein localization to cell periphery
positive regulation of neuron projection development
positive regulation of cell projection organization
organelle localization
neurotransmitter transport
neurotransmitter secretion
exocytosis
Golgi vesicle transport
Genes
E
Input
whole hypothalamic lysate
n.s.
adj. P-value < 0.05
Junb
Dusp1
AK081140
Btg2
Cebpd
AK084903
Pim3
Fos
A330076H08Rik
-Log10 P
Log2 fold change
F
Condition
Input CCK
Input Vehicle
IP: CCK
IP: Vehicle
IP: CCK
IP: Vehicle
Input: CCK
Input: Vehicle

Figure S2. Related to Figure 2: Chronic exposure to a HFHS diet impairs the electrical and transcriptional activation f PVN^{OT} neurons in response to peripheral CCK.

(A) Representative confocal micrographs of coronal brain sections from adult male OT:Ai14 reporter mice containing the PVN at the caudal (upper panel) and anteromedial (lower panel) level relative to bregma. Mice received fluorogold (FG; 15 mg/kg BW *i.p.*) 7 days prior sacrifice in order to label magnOT neurons, which form neurohemal contacts at the posterior pituitary (FG$^+$; blue). On the day of experiment, mice were injected with CCK (20 µg/kg BW *i.p.*) and consequent activation of PVN^{OT} neurons (green) was quantified by means of nuclear c-fos immunoreactivity (red). Scale bar, 50 µm.

(B) 3D rendered confocal scan of iDISCO-cleared coronal brain section from an adult male *OT:Ai14* reporter mouse spanning the entirety of the PVN (1 mm). Scale bar, 1 mm.

(C) Quantification of total c-fos$^+$ PVN^{OT} neuronal subpopulations from (A) differentiating between parvOT (FG$^-$) and magnOT (FG$^+$) subsets.

(D) GO enrichment analysis of DEG comparing IP of OT:RiboTag mice either fed SC diet or HFHS diet. Top enriched pathways number of DEG are indicated in the left panel, while the color indicates the adjusted p-value. Each pathway DEG are represented as dots, and plotted against log-fold changes, while the size indicates the adjusted p-values.

(E) Volcano plot highlighting the DEG in the input from OT:RiboTag mice fed SC diet receiving CCK (20 µg/kg BW *i.p.*) relative to vehicle.

(F) Heat map of sample-to-sample distance matrix for overall normalized gene expression read counts of both input and IP samples of OT:RiboTag mice fed either SC diet or HFHS diet that were additionally treated with either CCK (20 µg/kg BW *i.p.*) or vehicle. Euclidean distance clustering dendrograms are displayed above.

Figure S3

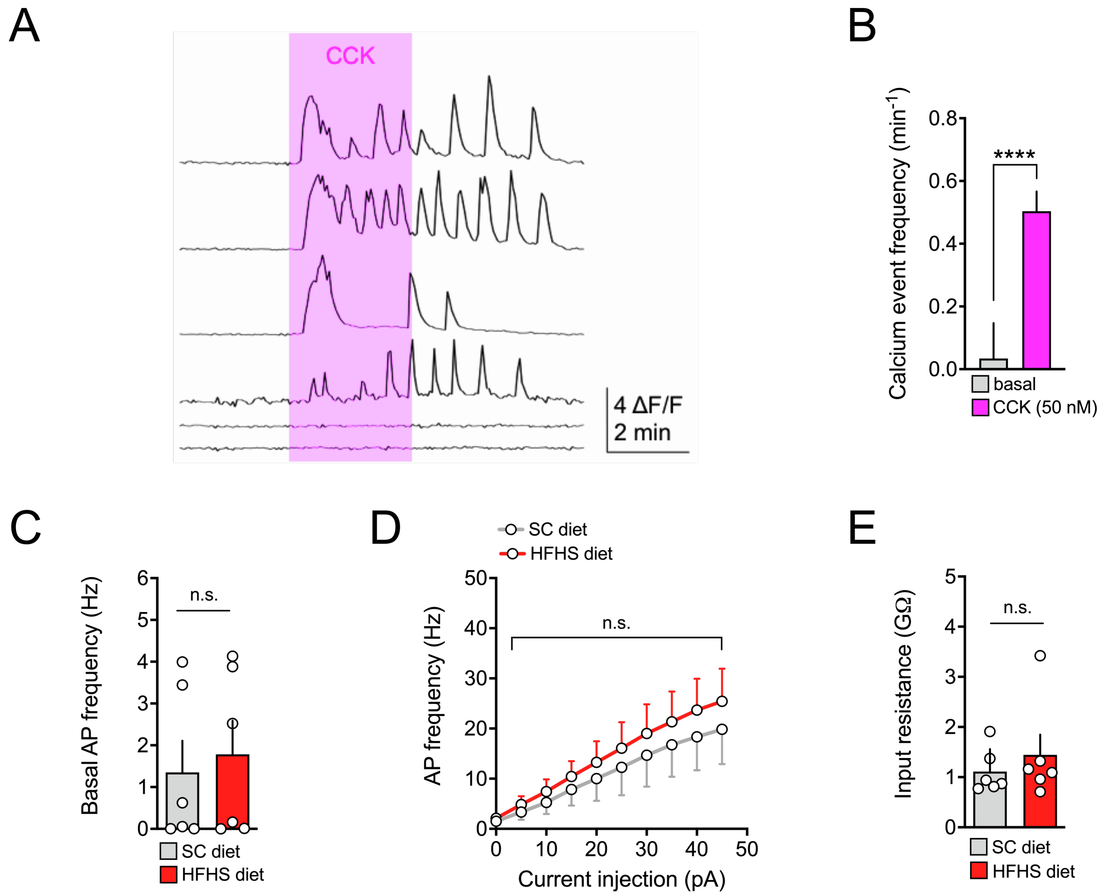

Figure S3. Related to Figure 3: PVN^{OT} neurons are activated by CCK *via* a direct, CCK$_A$R-dependent mechanism in lean but not obese mice.

(A) Cytosolic Ca^{2+} transients of individual PVN^{OT} neurons (lower panel) upon bath application of CCK (50 nM) in the presence of synaptic blockers.

(B) Quantification of Ca^{2+} event frequency as summary data of all imaged neurons. Data are presented as mean ± SEM. **** $P < 0.0001$. n = 1 mouse, 49 neurons (unpaired Student's *t*-test).

(C) Quantification of basal action potential frequency of putative magnOT neurons. Data are presented as mean ± SEM. n.s. = not significant. n = 2-3 mice/ 6 neurons per mouse (unpaired Student's *t*-test).

(D) Quantification of firing frequency as a function of injected current of putative magnOT neurons. Data are presented as mean ± SEM. n.s. = not significant. n = 2-3 mice/ 6 neurons per mouse (unpaired Student's *t*-test).

(E) Quantification of input resistance of putative magnOT neurons. Data is represented as mean ± SEM. n.s. = not significant. n = 2-3 mice/ 6 neurons per mouse (unpaired Student's *t*-test).

Figure S4

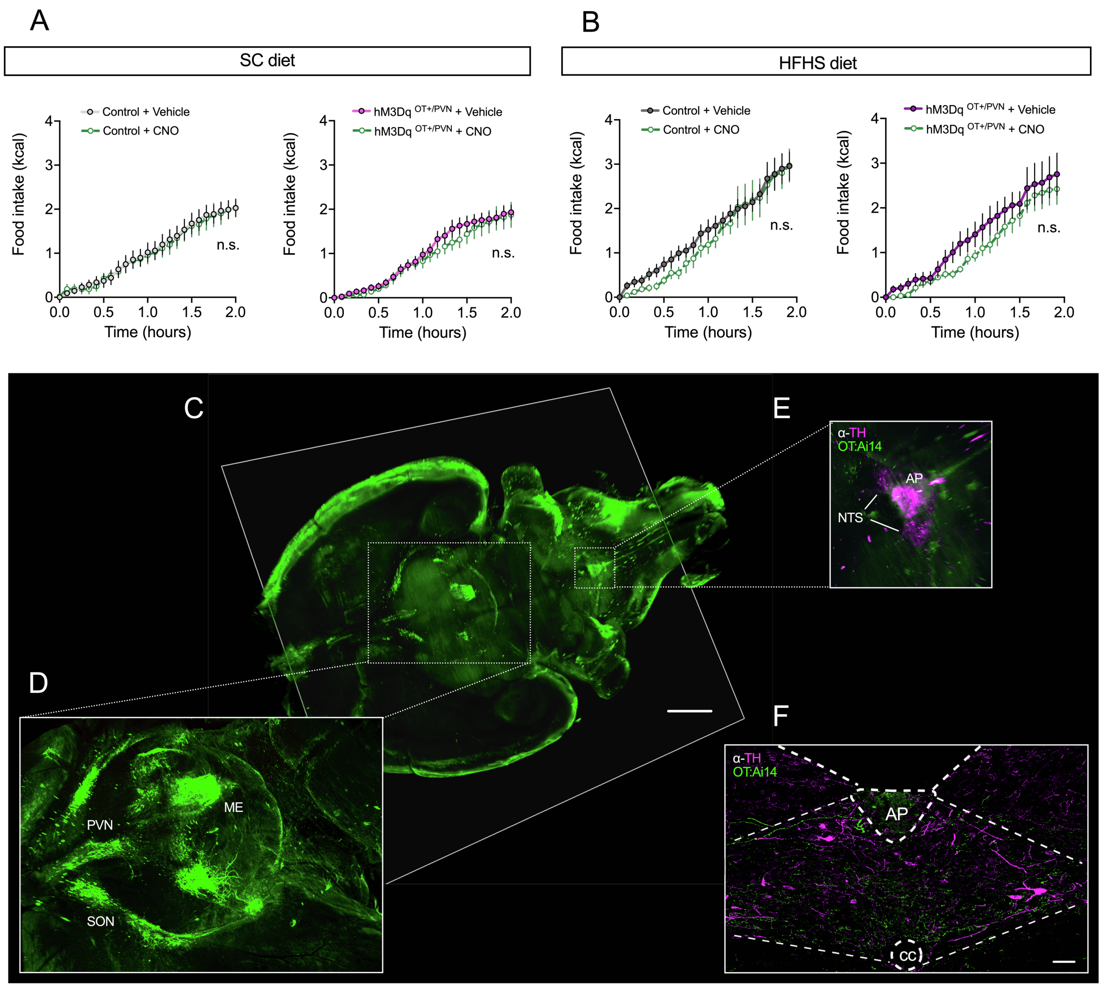

Figure S4. Related to Figure 4: Blunted suppression of food intake in response to CCK on a HFHS diet is reinstated by concomitant chemogenetic activation of PVN^{OT} neurons.

(A) Cumulative food intake of SC diet-fed mice nanoinjected with AAV-hSyn-DIO-mCherry (Control) or AAV-hSyn-DIO-hM3Dq-mCherry ($hM3Dq^{OT+/PVN}$) upon vehicle versus CNO (1 mg/kg BW *i.p.*). Data are presented as mean ± SEM. n.s. = not significant. n = 9 mice in a cross-over design (two-way ANOVA).

(B) Cumulative food intake of the same cohort of mice fed HFHS diet-fed for 6 weeks upon vehicle versus CNO (1 mg /kg BW *i.p.*). Data are presented as mean ± SEM. n.s. = not significant. n = 7-9 mice in a cross-over design (two-way ANOVA).

(C) 3D whole-brain image (horizontal view) of an iDISCO-cleared OT:Ai14 reporter mouse brain subjected to light-sheet fluorescence microscopy. Scale bar, 1 mm.

(D) 3D rendered zoom-in image (dashed line insert) of the hypothalamus showing the anatomical organization of the OT system.

(E) 3D rendered zoom-in image (dashed line insert) of the dorsal vagal complex (NTS and AP) in the brainstem containing catecholaminergic TH$^+$ neurons (magenta) and its innervation by OTergic fibres (green).

(F) Confocal micrograph of a coronal brain section of the NTS displaying catecholaminergic TH$^+$ neurons (magenta) and their innervation by OTergic fibres (green) at high resolution. Scale bar, Scale bar, 100 µm.

Figure S5

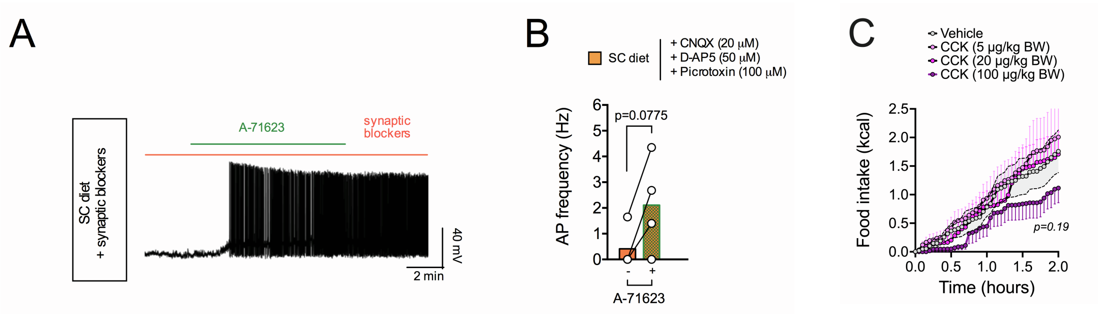

Figure S5. Related to Figure 5. Intersectional regulation of hypothalamic OT neurons by CCK_AR and κ-opioid receptors is dependent on dietary context.

(A) Representative traces of action potential frequency of magnOT neurons derived from adult male *OT:Ai14* reporter mice fed SC diet in response to bath-applied A-71623 (25 nM) pre-treated with synaptic blocker.

(B) Summary of changes in action potential frequency (right panel). Data are presented before and after application of A-71623 as mean ± SEM. n = 1 mouse/ 3 neurons per mouse (paired Students *t*-test).

(C) Cumulative food intake of HFHS diet-fed male C57BL/6J wildtype mice upon injection of low, medium, or high dose CCK (5, 20, and 100 µg/kg BW, respectively; *i.p.*) versus vehicle. Given that this experiment was run in conjunction with data presented in Figure 5H the same vehicle control group was used. Data are presented as mean ± SEM. n = 9 mice (two-way ANOVA).